MECH 6111 - GAS DYNAMICS

FALL 2024

COMPUTATIONAL FLUID DYNAMICS ANALYSIS OF A CONVERGING-DIVERGING NOZZLE

FINAL PROJECT REPORT

SUBMITTED TO

Professor: Dr. PIERRE Q GAUTHIER

Submitted by

PRATHMESH DEEPAK GONDKAR 40266289

ALLEN BRIGHTUS PRINCE 40304311

CONTENT

1. ABSTRACT

This study investigates the effects of varying back pressure on a nozzle operating under constant inlet conditions. The nozzle's performance is assessed based on outlet conditions corresponding to a given inlet pressure. For example, excessive exit pressure reduces thrust. As back pressure increases, the flow undergoes distinct stages, including choked flow, shock formation within the diverging section, shock at the nozzle exit, oblique shocks outside the nozzle, supersonic flow conditions, and expansion waves beyond the nozzle exit. Each of these phenomena is analysed in detail in subsequent sections. The simulations are conducted using ANSYS Fluent.

2. INTRODUCTION

The converging-diverging nozzle is a pivotal component in the field of aerospace engineering, designed to manage the flow of high-pressure fluids, typically gases such as air or exhaust. Its geometry comprises two distinct sections: a convergent portion where the cross-sectional area gradually decreases, and a divergent portion where the area expands. This strategic shape plays a vital role in propulsion systems, including jet engines and rocket nozzles, by effectively accelerating and controlling the fluid flow.

In the convergent section, the reduction in area causes the fluid velocity to increase as pressure decreases, following the principles of conservation of mass and energy. Upon reaching the throat—the narrowest point of the nozzle—the fluid often achieves sonic velocity (Mach 1). Beyond this point, in the divergent section, the fluid undergoes controlled expansion, transitioning to supersonic speeds while further reducing pressure. This mechanism enables efficient thrust generation and enhances the overall performance of propulsion systems.

This report delves into the computational fluid dynamics (CFD) analysis of flow through a converging-diverging nozzle. By employing numerical simulation methods, it aims to illustrate and quantify variations in velocity, pressure, and Mach number throughout the nozzle. The findings provide a comprehensive understanding of shockwave dynamics, energy transformations, and their implications for practical engineering applications.

3. PURPOSE AND SCOPE

The primary purpose of this study is to design and analyze a converging-diverging nozzle to investigate various flow phenomena, including subsonic choked flow, the formation of a normal shock in the divergent section, the occurrence of oblique shocks, and the presence of expansion waves outside the nozzle. These phenomena are critical for understanding the complex interplay of velocity, pressure, and density changes within the nozzle, which directly affect the efficiency and performance of propulsion systems.

This analysis employs a dual-method approach that combines computational fluid dynamics (CFD) simulations using ANSYS software with theoretical one-dimensional calculations. By leveraging CFD, the study provides detailed visualizations and quantitative insights into the flow characteristics, such as velocity gradients and pressure distributions. The theoretical calculations offer a baseline for comparison, enabling the validation of simulation results and uncovering any deviations due to practical considerations or numerical approximations.

Through this comprehensive approach, the study seeks to bridge the gap between theoretical fluid dynamics and practical applications. The findings aim to not only validate the design parameters of the nozzle but also inform potential improvements in its geometry for enhanced performance. Furthermore, the research explores the behavior of flow under various operational conditions, providing valuable insights for optimizing nozzle designs in aerospace and industrial applications. Ultimately, the scope of this study extends beyond validation, contributing to the broader understanding of fluid dynamics in high-speed systems and guiding the development of efficient propulsion technologies.

4. METHODOLOGY

A convergent-divergent nozzle is designed to investigate various flow phenomena under constant inlet pressure. Analytical calculations determine the back pressure required for specific flow conditions. To simplify the study, the flow is assumed to be steady, two-dimensional, and inviscid, modelled as planar with a unit depth. The nozzle geometry is tailored to achieve a target Mach number, with the throat size fixed and the inlet and exit heights calculated accordingly.

The design and analysis procedure includes:

1. Geometry Design: Using ANSYS Design Modeler to create the nozzle shape.
2. Mesh Generation: Implementing face meshing to ensure accurate flow resolution.
3. Simulation: Setting up and solving flow conditions in ANSYS Fluent.
4. Comparison: Validating the simulated results against analytical solutions derived from one-dimensional calculations.

This approach ensures a comprehensive understanding of nozzle performance under various operating conditions. Once the simulation results are obtained, they are compared against analytical solutions derived from one-dimensional flow equations. This comparison serves as a validation step, ensuring that the numerical outcomes align with theoretical expectations. Any discrepancies are analyzed to understand potential limitations or assumptions influencing the results. This methodology provides a robust framework for evaluating the performance and efficiency of the converging-diverging nozzle under varying operational scenarios.

5. GEOMETRY

The geometric design parameters for the nozzle in this study are outlined below. All dimensions are in millimetres.

Design Parameters:

- **Inlet Mach Number (M_inlet):** 0.2
- **Exit Mach Number (M_exit):** 2.5
- **Throat Height:** 10 mm

Calculations:

1. **Inlet Height:**
    - From the Isentropic Flow Table,

      M=0.2 and $A/A^* = 2.96352$
    - Since the flow depth is unitary, this ratio corresponds directly to the ratio of heights.
    - Using Inlet Height=A/A∗×Throat Height:-

      Inlet Height=2.96352×10=29.6352mm.
2. **Exit Height:**
    - From the Isentropic Flow Table, for

      M=2.5M, and $A/A^* = 2.6367$
    - Using Exit Height=A/A∗×Throat Height:-

      Exit Height=2.6367×10=26.367mm

Nozzle Dimensions:

- **Total Length of the Nozzle:** 180 mm
- **Position of the Throat from the Inlet:** 60 mm

his geometry forms the foundation for analysing the flow phenomena under various conditions in the nozzle.

The dimensions are summarized in the table below:

DIMENSIONS (mm)	
Inlet Height (H1)	29.635
Throat Height (H2)	10.0
Exit Height (H3)	26.367
Throat Position (L1)	5.0
Total Length (L2)	60.0
Extended Length (L3)	180.0

Table 5.1 Geometry Dimensions

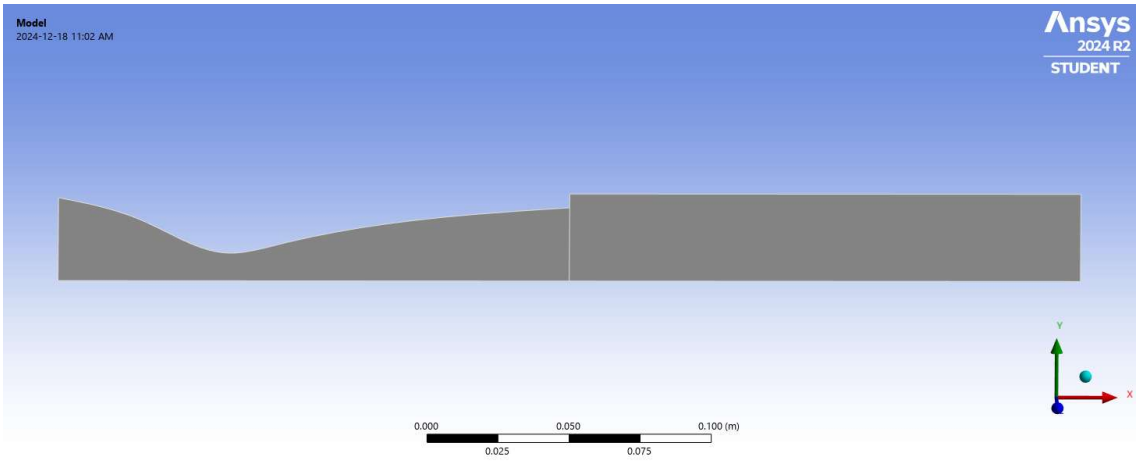

Figure 5.1 Geometry in Design Modeler

6. MESHING

The Computational Domain (C-D) Nozzle, integrated with a tank, was structured into 25,400 finite elements to investigate the flow characteristics under different conditions. These conditions included Subsonic Choked Flow, Supersonic Flow, Normal Shock within the Divergent Section, Oblique Shock outside the Nozzle, and Expansion Waves outside the nozzle, which will be monitored within the tank.

To ensure an accurate representation of flow behaviour, the inlet and outlet sections of the nozzle were subdivided into 40 segments each. Bias factors of 3.0 were applied strategically to the inlet wall and the outlet tank region to refine the resolution in these critical areas, where significant flow gradients are expected. Given the symmetry of the nozzle design, only one-half of the nozzle geometry was modelled for computational efficiency, significantly reducing the overall computational cost without sacrificing accuracy in the results.

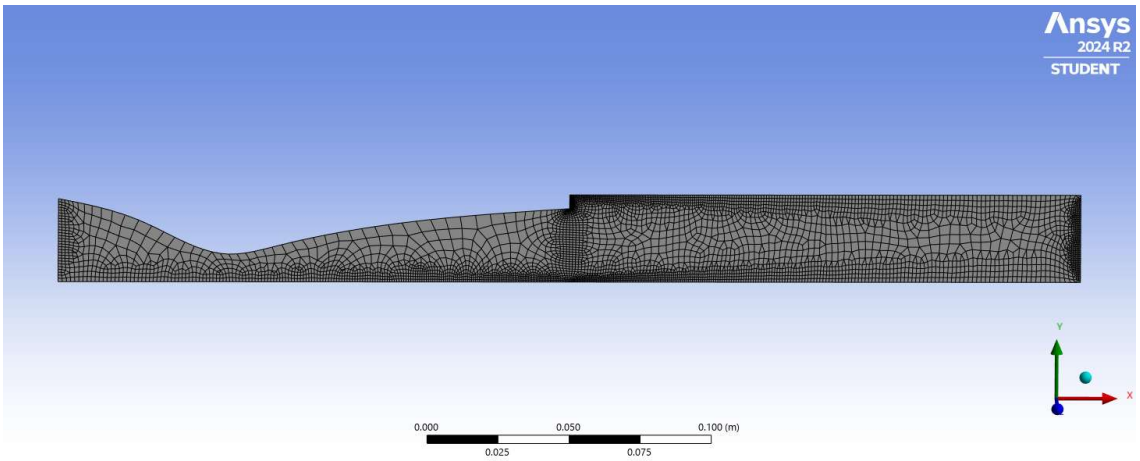

Figure 6.1 Meshing

7. SIMULATION

In the Fluent simulation setup window, the essential conditions for the analysis were specified and executed. The solver was set to a density-based approach with a planar geometry configuration to accommodate the flow dynamics in the nozzle and tank system. The energy equation was activated, assuming the flow to be inviscid and steady, which simplified the calculations while still providing useful insights into the overall flow behaviour.

Boundary conditions at the inlet were defined using total pressure and total temperature, ensuring an accurate representation of the incoming flow characteristics. For the outlet, back pressure was adjusted across different flow conditions to examine its effect on flow behaviour and performance under varying scenarios.

The necessary solution controls were applied to ensure convergence and accuracy of the results. After completing the setup, the simulation was executed, capturing various flow outcomes such as pressure, velocity profiles, shock interactions, and wave patterns. These results will be thoroughly analysed and discussed in the following section.

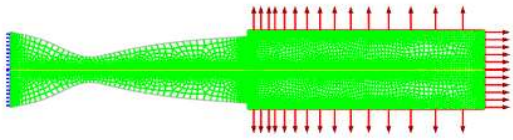

Figure 7.1 Simulation

8. CALCULATIONS

The isentropic flow and normal shock tables for an ideal gas (γ = 1.4) are used to do the theoretical calculations. The subscript 'i' indicates the inlet condition, 'e' indicates the exit condition, '*' represents the throat conditions, and 'b' represents the after-exit conditions. The total temperature is constant in all type of flows.

Variable	**Symbol**	**Unit**
Pressure	P	Pascal (Pa)
Temperature	T	Kelvin (K)
Total Temperature	T	Kelvin (K)
Total Pressure	P	Pascal (Pa)
Mach Number	M	-
Area	A	-
Height	H	mm

Table 8 Units and variables

8.1. Inlet Conditions ($M_i = 0.2$)

The total pressure and total temperature are taken as

$$P = 101325\ Pa \ and \quad T = 300K$$

Taking data from the IST table we get,

$P/P_0 = 0.9724967$, $T/T_0 = 0.9920634$

The calculated inlet properties are listed below:

Inlet Conditions				
M	P	T	P	T
0.2	98538.22 Pa	297.6 K	101325 Pa	300 K

Table 8.1 Theoretical inlet Conditions

8.2. At Throat ($M^* = 1$)

From the IST table, for M=1

P/P_0 = 0.5283, T/T_0= 0.8333

The calculated throat properties are listed below:

Throat Conditions				
$M*$	$P*$	T^*	P_0	T_0
1	52523 Pa	250 K	101325 Pa	300 K

Table 8.2 Theoretical Throat Conditions

8.3. For Subsonic Flow condition: Choked Condition

For A / A*=2.6, in the subsonic region, we get the following values for choked flow from the IST table,

M_e= 0.22, P/P_0 = 0.96496475, T/T_0= 0.98986210

The choked flow properties are listed below:

Choked Conditions				
M_e	P_e	T_e	P_0	T_0
0.22	97775 Pa	296.95	101325	300

Table 8.3Theoretical Choked Conditions

8.4. For Supersonic flow: Design Conditions

From IST, data for design Mach pressure

M_e= 2.5 are P/P_0 = 0.05853, T/T_0 = 0.44

Supersonic Design Conditions				
M	P	T	P	T
2.5	5930.25	133.2	101325	300

Table 8.4 Theoretical Supersonic Design Conditions

8.5. Assuming Normal Shock at Exit Plane

M_x= 2.5, P_x= 5930.54

From NST $M_y = M_e$ = 0.513 $and\ P/P_0$ = 7.125, T_y/T_x = 2.1375, P_{0y}/P_{0x} = 0.499

Therefore, the after-shock values at exit are:

Normal Shock at Exit Conditions				
M_e	P_e	T_e	P_0	T_0
0.513	42253.05 Pa	282.15K	50662.5	300

Table 8.5 Theoretical Normal Shock at Exit Conditions

8.6. Normal Shock Inside the Nozzle (For back pressure 50000 Pa)

By using the continuity equation between throat and exit,

$$\rho^* A^* V^* = \rho A_e V_e$$

$$M = 0.4285$$

From IST, M_e = 0.4285 , we can find T_e= 289.4K, P_{02} = 56726.86 Pa, which gives

$$P_{02}/P_{01}=0.56$$

From NST table using above ratio, we can say M= 2.35, M= 0.52

After Shock				
M_e	P_e	T_e	P_0	T_0
0.4285	50000 Pa	289.4 K	56726.86 Pa	300 K

Table 8.6Theoretical Exit Condition after Normal Shocks

Before and Aftershock conditions					
M_x	M_y	P_x	P_y	T_x	T_y
2.35	0.52	7493.7 Pa	47032.3 Pa	142.5 K	283.57K

Table 8.7 Theoretical Across Normal Shock Conditions

8.7. Oblique Shock Outside the Nozzle

$$P_b/P_e=1.18$$

Taking data from the NST table, we get

For M = 1.075, we get M= M= 0.932

θ = 25.4675, δ = 2.547

$M_2=M_{2n}/Sin(\theta - \delta)$ =2.39

After Oblique Shock Conditions		
M	P	T
2.39	7000 Pa	139.7 K

Table 8.8 Theoretical After Oblique Shock Conditions

8.8. Expansion Wave Outside the Nozzle (P_b = 3000 Pa)

For expansion wave P_b/P_{01} = 0.0296, corresponding Mach number M = 2.94 and temperature T=109.5 K from IST table.

After Expansion Wave Conditions		
M	P	T
2.94	3000 Pa	109.5 K

Table 8.9 Theoretical After-Expansion conditions

9. Results And Discussion

9.1. Subsonic Choked Flow Condition:

The choked flow back pressure was found to be 97,775 Pa. At this pressure, the flow reaches sonic conditions at the throat and then decelerates as it exits the nozzle.

Mach Number

The Mach number reaches M=1 at the throat and gradually decreases in the diverging section, as shown in the figure and graph below.

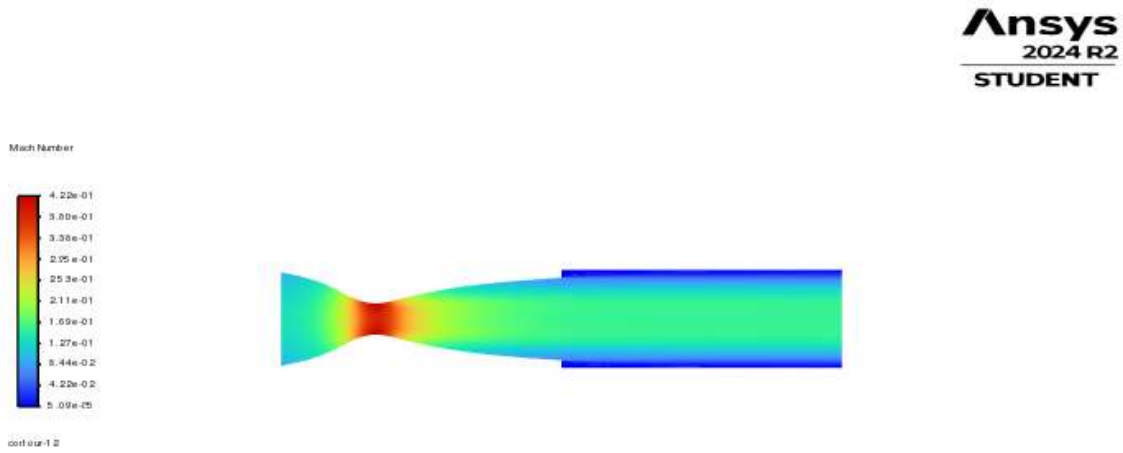

Figure 9.1 Contour of Mach number for choked flow.

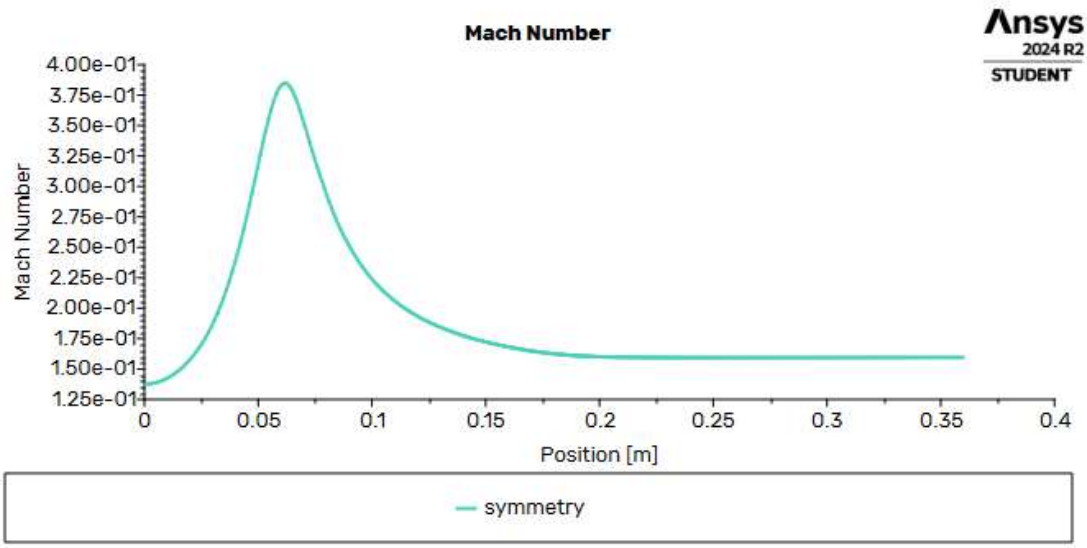

Figure 9.2 Mach Number vs Position graph for choked flow

Static Pressure:

The figure below depicts the Static Pressure contour across the nozzle and tank geometry. This contour map visually represents the pressure distribution within the flow domain, emphasizing regions with notable pressure changes due to various flow conditions, including shock waves and expansion zones.

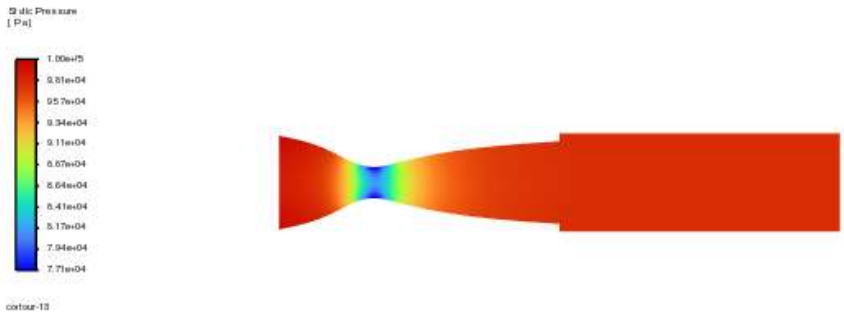

Figure 9.3 Contour of Static Pressure for Choked Flow

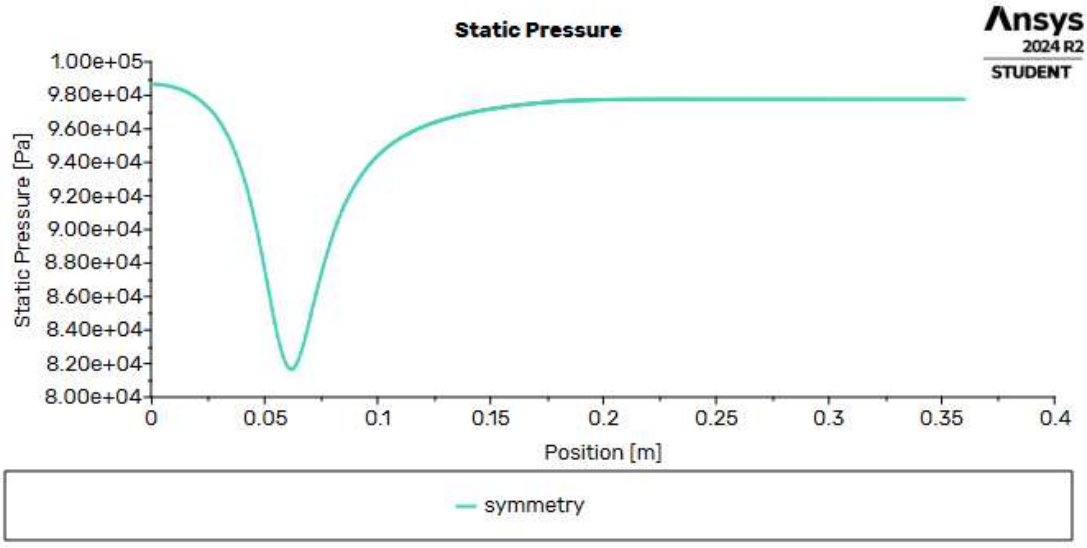

Figure 9.4 Static Pressure vs Position graph for Choked flow

Static Temperature:

The figure below displays the contour of Static Temperature across the geometry of the nozzle and tank system. The temperature distribution reflects the thermal changes occurring within the flow, particularly at areas where shocks, expansion waves, and flow transitions take place. This visualization provides insight into how temperature varies throughout the nozzle and tank regions under different flow conditions.

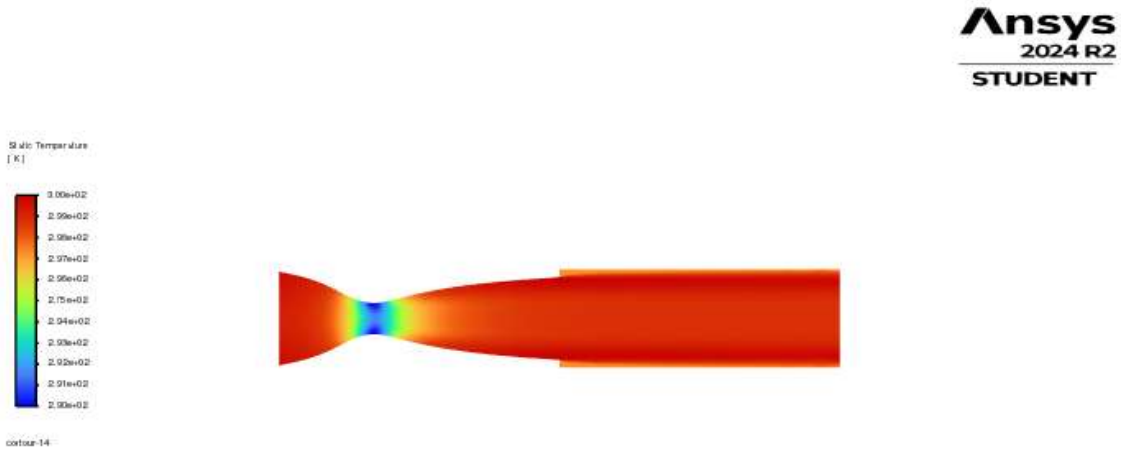

Figure 9.5 Contour of Static Temperature for Choked Flow

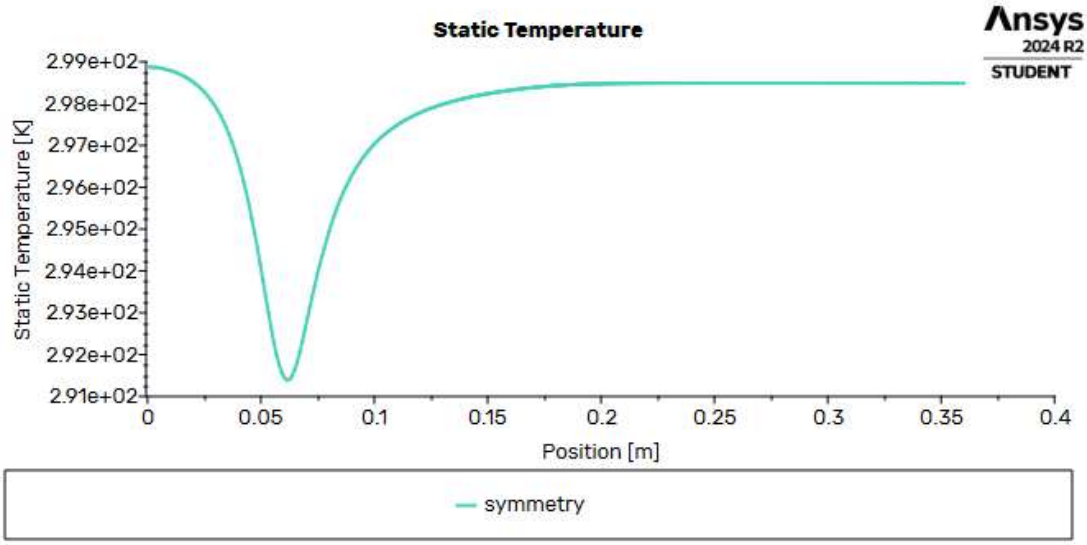

Figure 9.6 Static Temperature vs Position graph for Choked flow

Comparison:

The table below presents a comparison between the simulation results and the analytical 1-D calculations for key flow parameters. The Mach number and static temperature values from the simulation exhibited a discrepancy of less than 1% compared to the theoretical values, indicating good agreement between the simulation and the 1-D analytical model.

However, it was observed that the Mach number at the exit of the nozzle was 5% lower than the calculated value from the 1-D analysis. This deviation may be attributed to factors such as the approximation of inviscid flow, assumptions in the boundary conditions, or the influence of external flow interactions that are not accounted for in the 1-D model.

The comparison highlights the accuracy of the simulation in capturing the overall flow behaviour while identifying areas where further refinement or investigation could be beneficial.

Choked Flow			
Parameter	Analytical	CFD	Error %
	Exit	Exit	
Me	0.226	0.215	4.9
Pe	97775	96876.4	0.9
Te	296.95	296.189	0.3
	At Throat	At Throat	
$M*$	1	0.99	1
$P*$	52523	52237.3	0.5
$T*$	250	250.041	0

Table 9.1 Comparison between Analytical and Simulated results (Choked Flow)

9.2. Super Sonic Design Flow Condition:

As detailed in our calculations, the theoretical Super Sonic design back pressure was determined to be 5930.25 Pa. At this pressure, the flow is expected to reach the design Mach number of M = 2.5.

Mach Number

The figure below illustrates the contour of Mach number throughout the geometry of the nozzle and tank system. The Mach number distribution reveals the acceleration and deceleration of the flow as it passes through the nozzle, with particular emphasis on the transition from subsonic to supersonic flow.

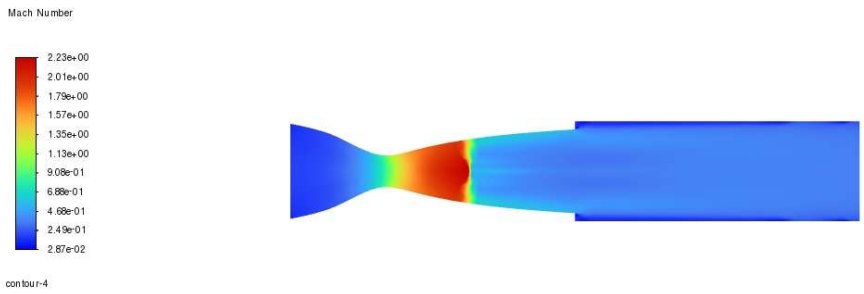

Figure 9.7 Contour of Mach number for Supersonic Flow Conditions

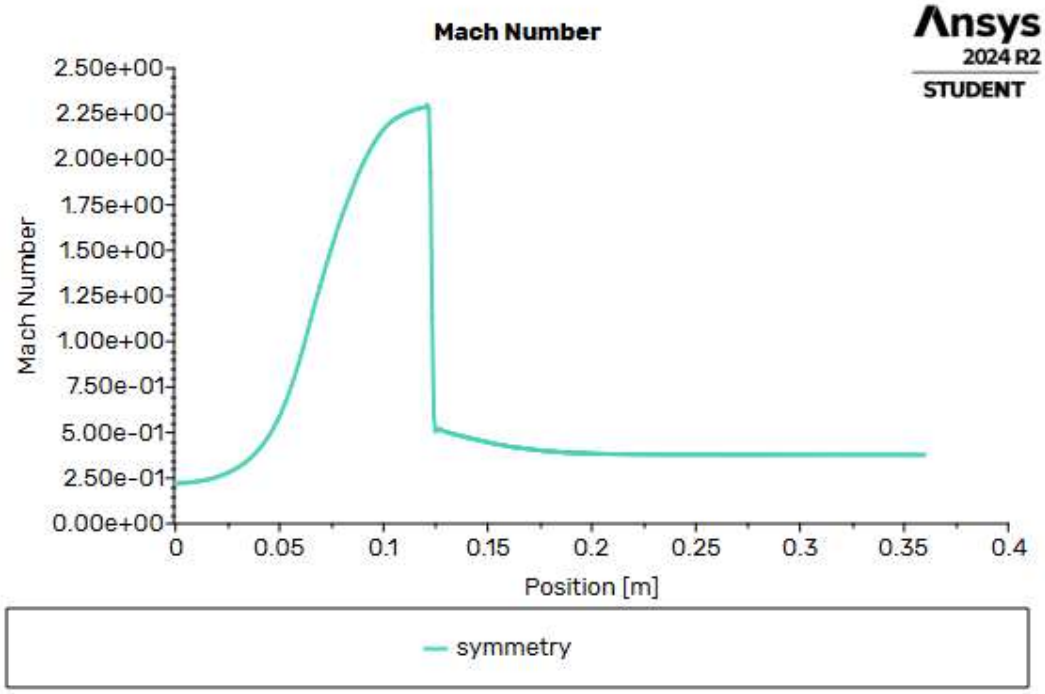

Figure 9.8 Mach Number vs Position graph for Supersonic flow Conditions

Static Pressure:

The figure presents the Static Pressure contour across the geometry, providing a visual representation of pressure distribution throughout the flow domain. Additionally, a Static Pressure vs. Position graph along the symmetry axis is shown for analysis, illustrating how static pressure changes at various locations within the nozzle and tank system. This graph helps interpret the pressure variation along the flow path.

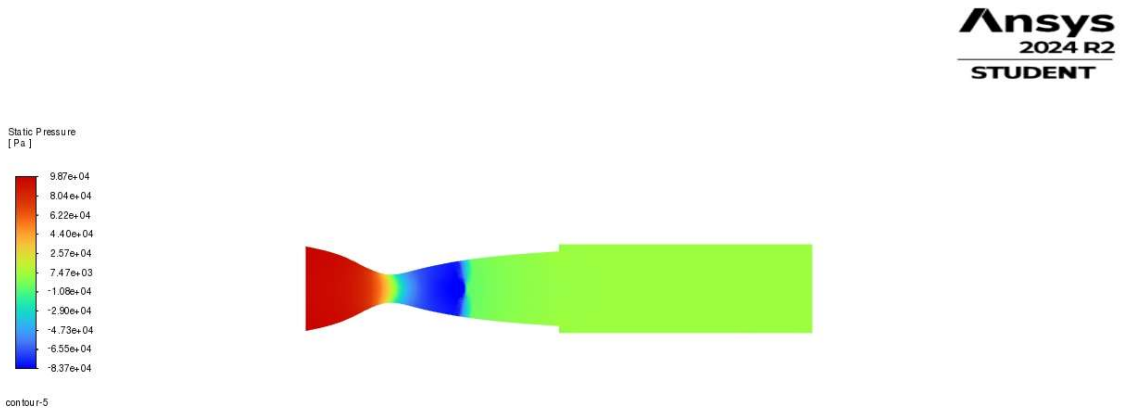

Figure 9.8 Contour of Static Pressure (Supersonic Design)

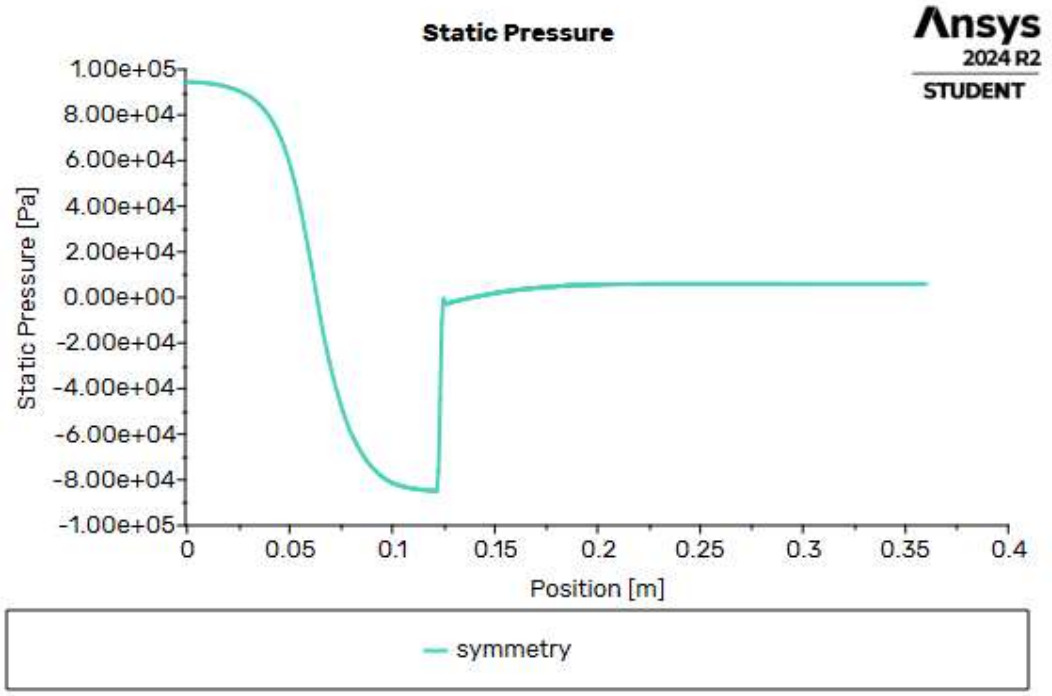

Figure 9.9 Static Pressure vs Position Graph (Supersonic Design)

Static Temperature:

The figure below displays the Static Temperature contour across the geometry of the nozzle and tank system under the supersonic design flow condition. The contour map illustrates the thermal distribution throughout the flow domain, highlighting regions of temperature change due to the supersonic flow and shock interactions.

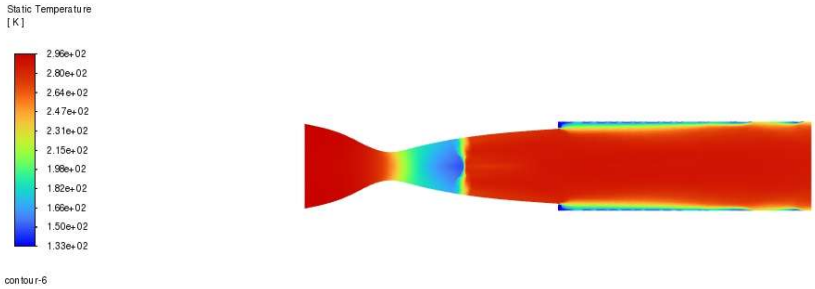

Figure 9.10 Contour of Static Temperature for Supersonic Design

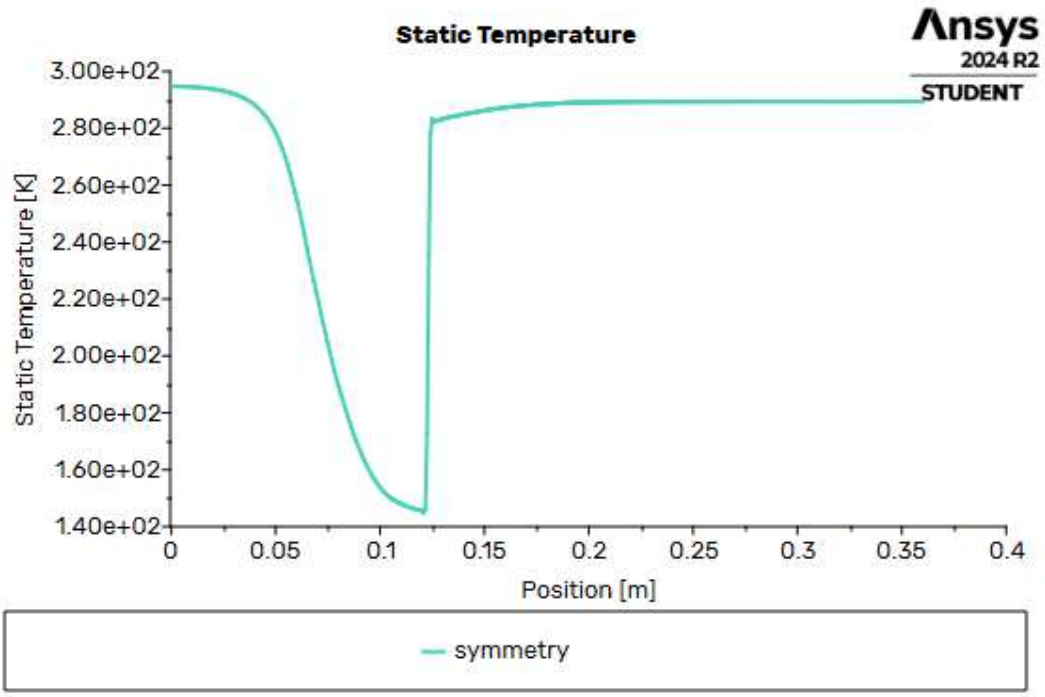

Figure 9.11 Static Temperature vs Position graph for Super Sonic Design

Comparison:

The table below presents a comparison between the CFD results and the analytical 1-D calculations. The Mach number and static temperature values exhibited an error of less than 1% when compared to the theoretical values. However, the static pressure at the exit was found to be 3.5% lower than the calculated design exit pressure.

Super Sonic			
Parameter	Analytical	CFD	Error %
	Exit	Exit	
Me	2.5	2.5217	0.9
Pe	5930.25	5722.34	3.5
Te	133.2	132.238	0.7

Table 9.2 Comparison between Analytical and Simulated results (Supersonic Flow)

9.3. Normal Shock in Diverging Section (Pb = 50000 Pa)

From the calculations in Section 7.5, it was determined that for this design, a normal shock will occur at the exit when the back pressure P=42,253.05 Pa. Therefore, a back pressure range of 42,253 < P < 97,775 will result in a normal shock in the diverging section of the nozzle. For simulation purposes, a back pressure of P=50 kPa was chosen to model the normal shock in the diverging section.

Mach Number:

The figure illustrates the Mach number contour across the geometry of the nozzle and tank system. A Mach number vs. Position graph along the symmetry axis is also presented for analysis, helping to interpret the variation of Mach number at different positions within the flow domain.

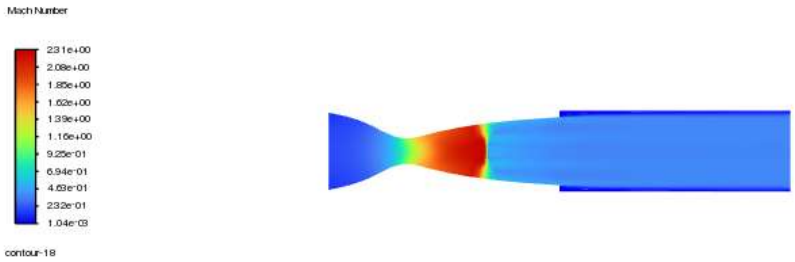

Figure 9.12 Contour of Mach number for Normal Shock

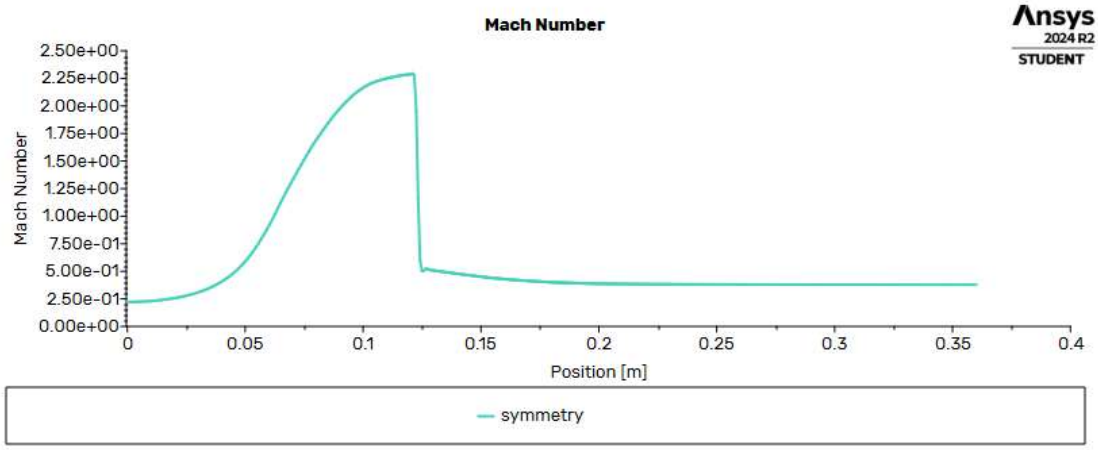

Figure 9.13 Mach Number vs Position Graph for Normal Shock

Static Pressure:

The figure presents the Static Pressure contour across the geometry, providing a visual representation of pressure distribution throughout the flow domain.

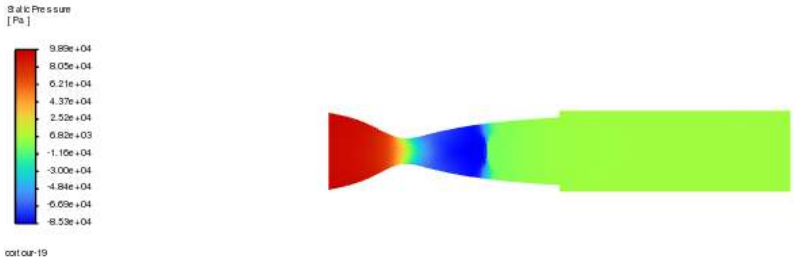

Figure 9.14 Contour of Static Pressure for Normal Shock

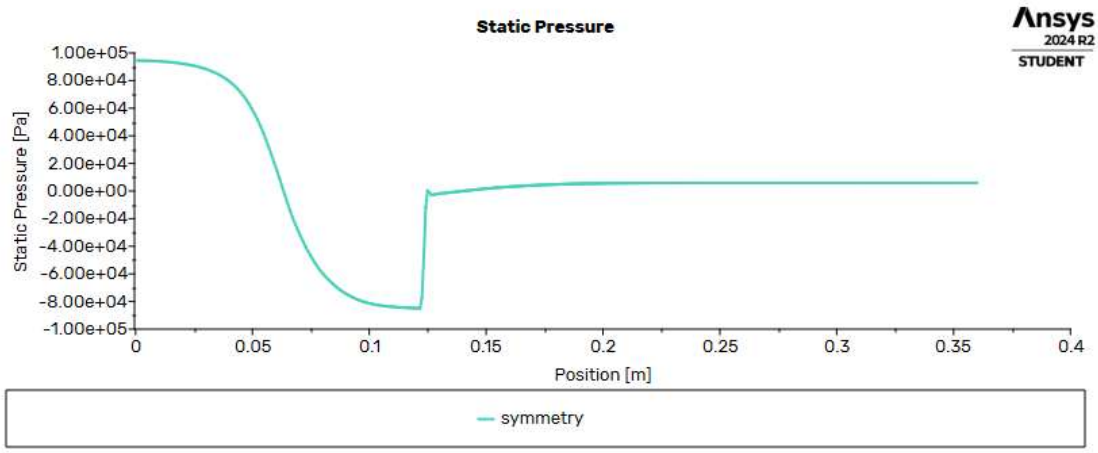

Figure 9.15 Static Pressure vs Position graph for Normal shock

Static Temperature:

The figure presents the Static Temperature contour across the geometry of the nozzle and tank system. Additionally, a Static Temperature vs. Position graph along the symmetry axis is included for interpretation, showing how static temperature varies at different positions within the flow domain.

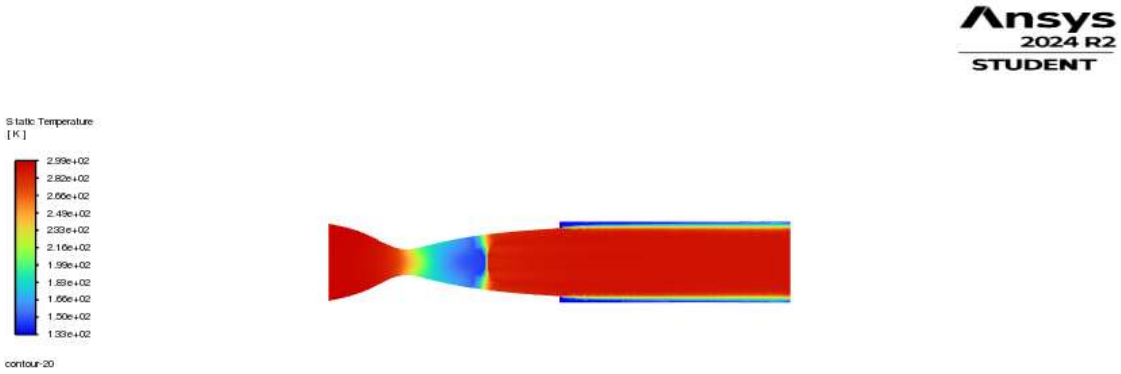

Figure 9.16 Contour of Static Temperature for Normal Shock

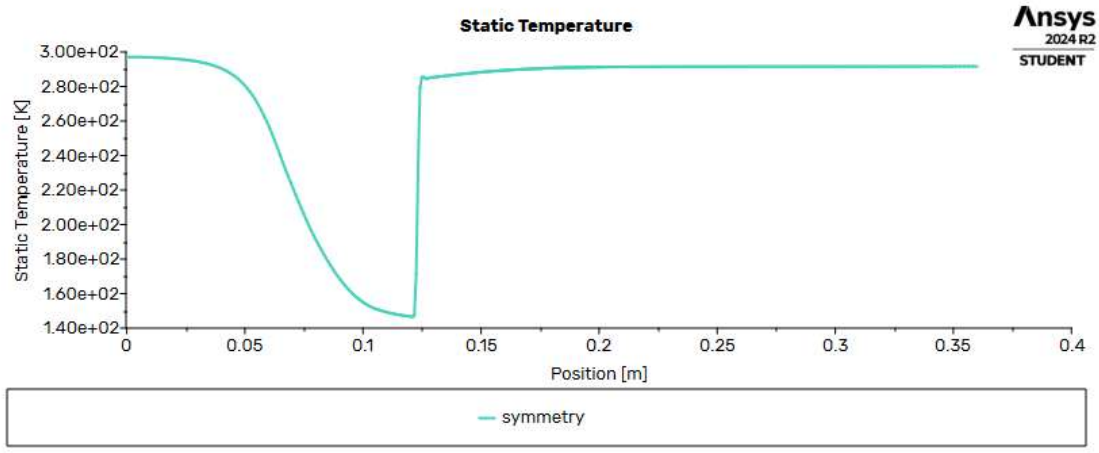

Figure 9.17 Static Temperature vs position for Normal Shock

Total Pressure:

The figure displays the Total Pressure contour across the geometry of the nozzle and tank system. A Total Pressure vs. Position graph along the symmetry axis is also provided for interpretation, illustrating how total pressure changes at various positions within the flow domain.

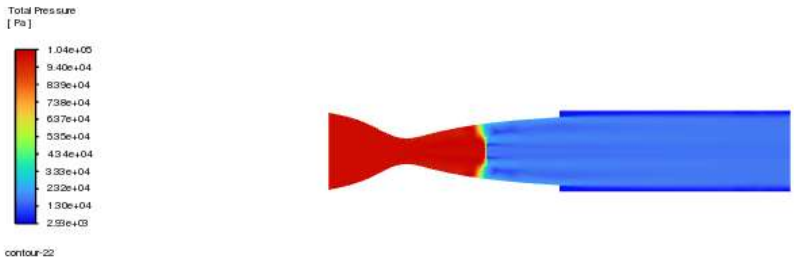

Figure 9.18 Contour of Total Pressure for Normal Shock

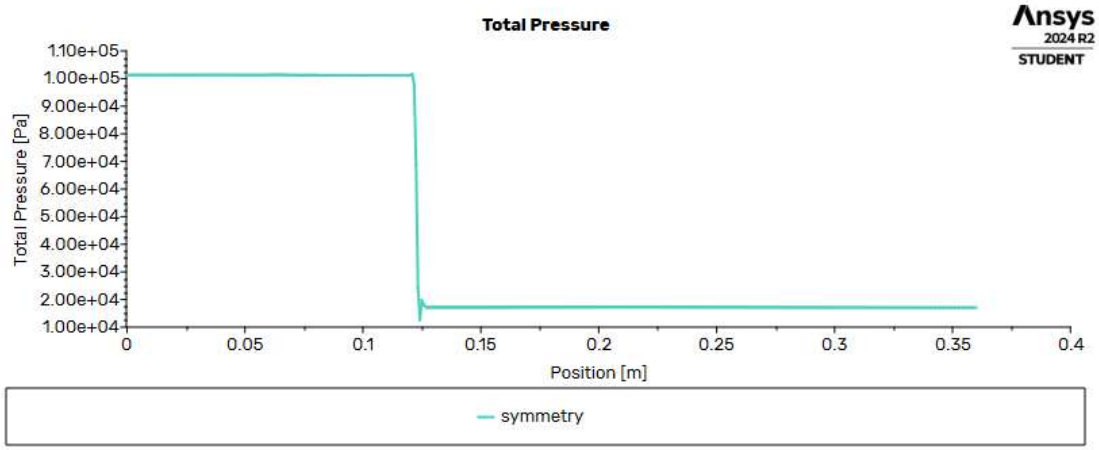

Figure 9.19 Total Pressure vs Position for Normal Shock

Comparison:

The theoretical values for P=50 kPa are compared with the CFD results in the table below. With the exception of the exit Mach number, all other parameters exhibited minimal deviation from the theoretical values. The normal shock was observed at a distance of 85 mm from the throat.

Normal Shock on the Diverging Section			
Parameter	Analytical	CFD	Error %
	Exit	Exit	
M_e	0.4285	0.541956	26.5
Pe	45000	47642.8	4.7
Te	289.4	284.492	1.7
	Before Shock	Before Shock	
Mx	2.35	2.4072	2.4
Px	7493.7	6836.96	8.8
Tx	142.5	139.134	2.4
P_{0x}	101325	101095	0.2
	After Shock	After Shock	
My	0.52	0.537193	3.3
Py	47032.3	46404.6	1.3
Ty	283.575	280.085	1.2
P_{0x}	56726.8	56461	0.5

Table 9.3 Comparison between Analytical and Simulated results (Normal Shock)

4. Oblique Shock ($Pb = 7000Pa$)

From our calculations, it was determined that a normal shock occurs at the exit when P=42,253.05 Pa. Any pressure between this value and the design pressure will result in an oblique shock. For demonstration purposes, P=7,000 Pa was chosen to simulate an oblique shock.

Mach Number:

The figure below shows the distribution of Mach number across the geometry, along with a graph that plots MachJJ number versus position along the symmetry line for further analysis.

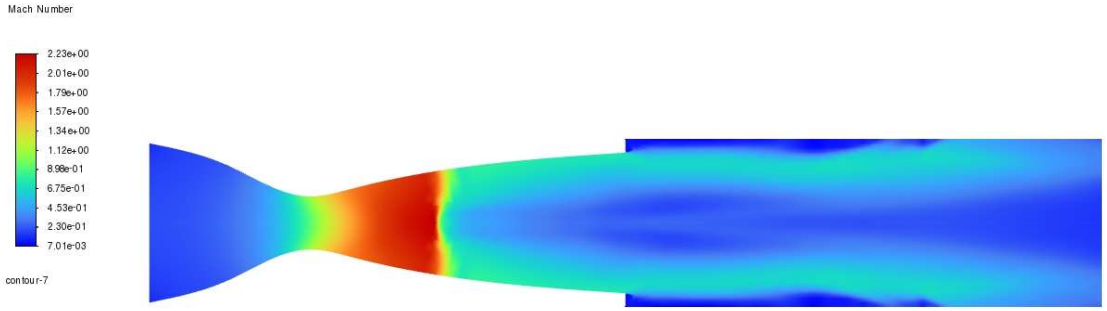

Figure 9.19 Contours of Mach Number for Oblique Shock

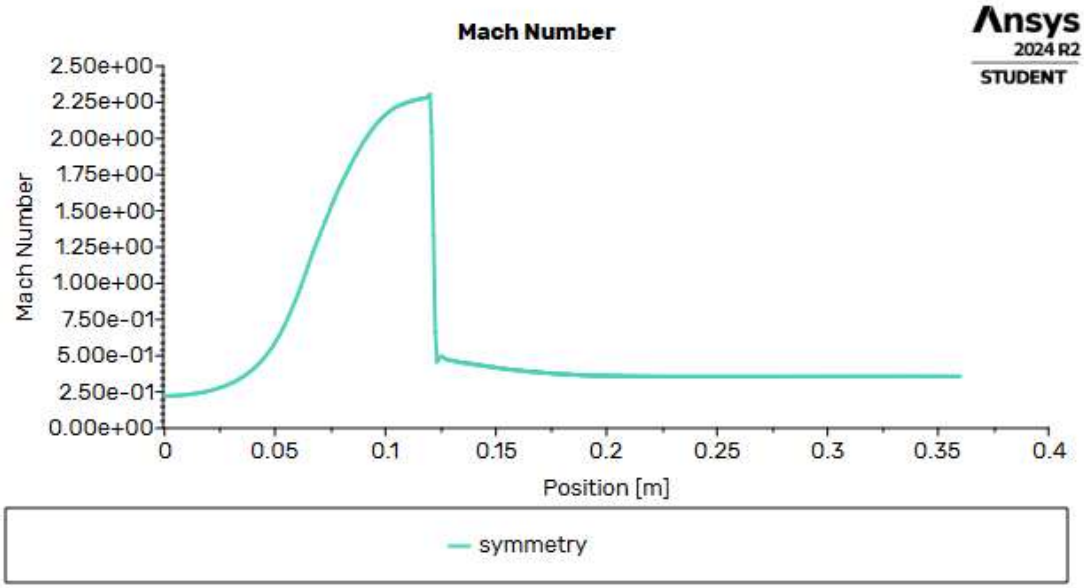

Figure 9.20 Mach Number vs Position(Oblique Shock)

Static Pressure:

The diagram depicts the distribution of static pressure within the geometry, along with a graph that plots static pressure versus position along the symmetry line for analysis.

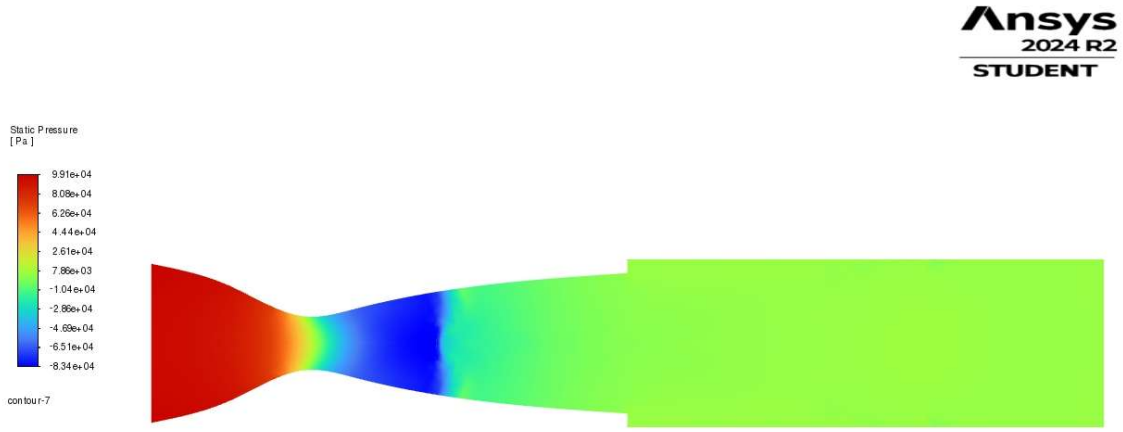

Figure 9.21 Contours of Static Pressure for Oblique Shock

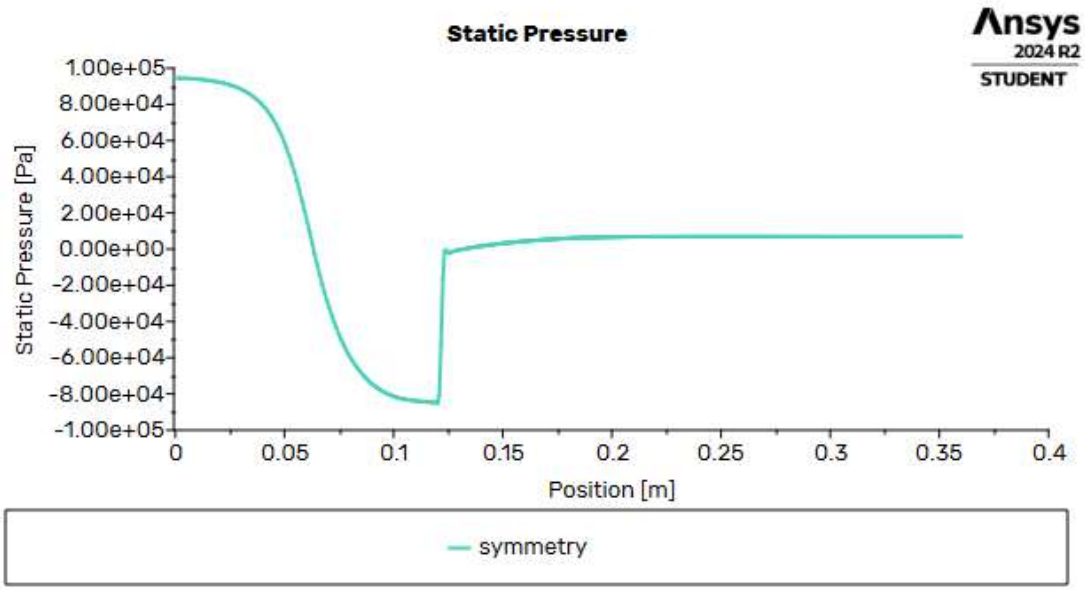

Figure 9.22 Static Pressure vs Position graph(Oblique Shock)

Static Temperature:

The figure below presentJs the contour of static temperature across the geometry, accompanied by a graph that plots static temperature versus position along the symmetry line for interpretation.

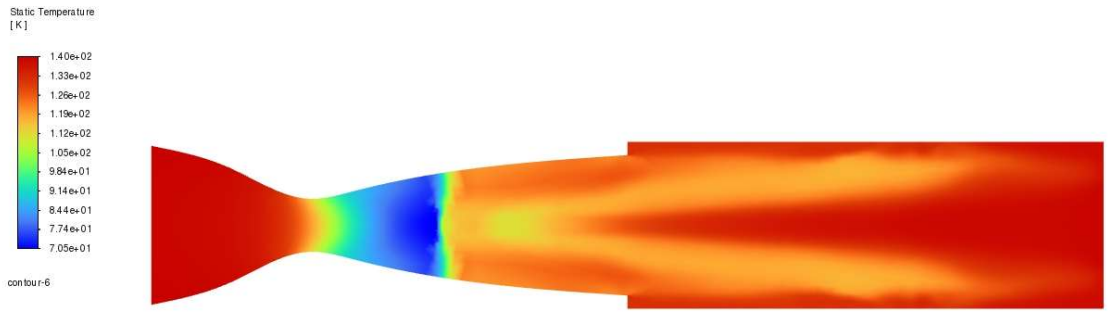

Figure 9.23 Contours of Static temperature (Oblique Shock)

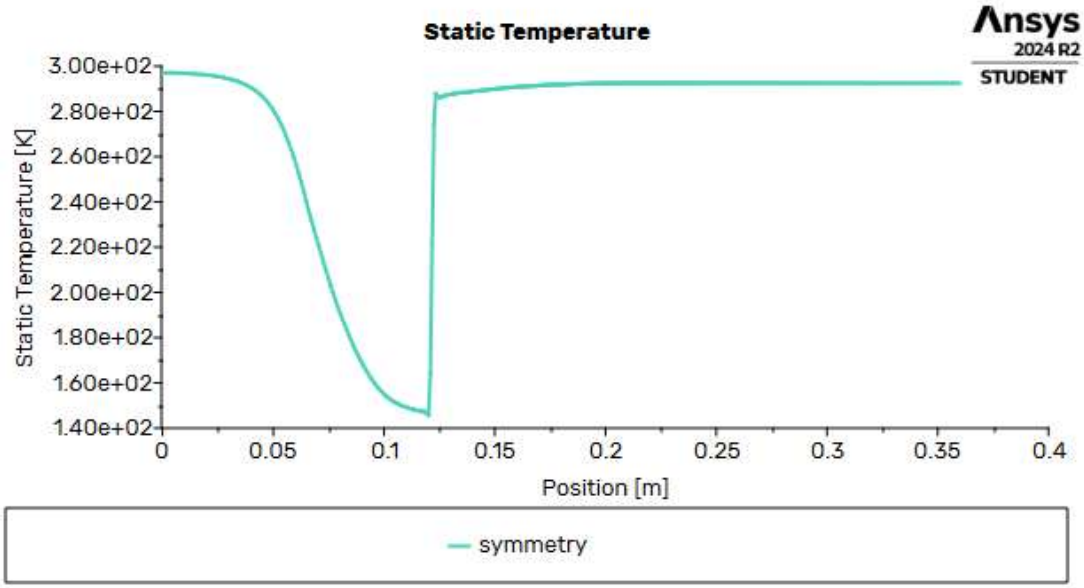

Figure 9.24 Static Temperature vs Position graph(Oblique Shock)

Comparison:

The table below compares the analytical values with the simulated results. The CFD results show minimal deviation from the analytical solution. The Mach number after the first oblique shock was found to be 2.38.

Oblique Shock			
Parameter	Analytical	CFD	Error %
	Exit	Exit	
Me	2.5	2.5217	0.9
Pe	5930.25	5722.34	3.5
Te	133.2	132.238	0.7
	After Shock	After Shock	
Mb	2.39	2.38	0.4
Pb	7000	7109.73	1.6
Tb	139.7	140.68	0

Table 9.4Comparison between Analytical and Simulated results (Oblique Shock)

5. Expansion Waves

If the back pressure is lower than the design exit pressure, the flow will expand to match the back pressure, resulting in a higher Mach number after the expansion wave. For demonstration purposes, P=3 kPa is used.

Mach Number:

The figure below shows the Mach number distribution within the geometry, along with a graph plotting Mach number versus position along the symmetry line for analysis. As observed from the contours, the gas expands after exiting the nozzle. However, due to the presence of the tank, the flow direction changes, resulting in the formation of a shock within the tank.

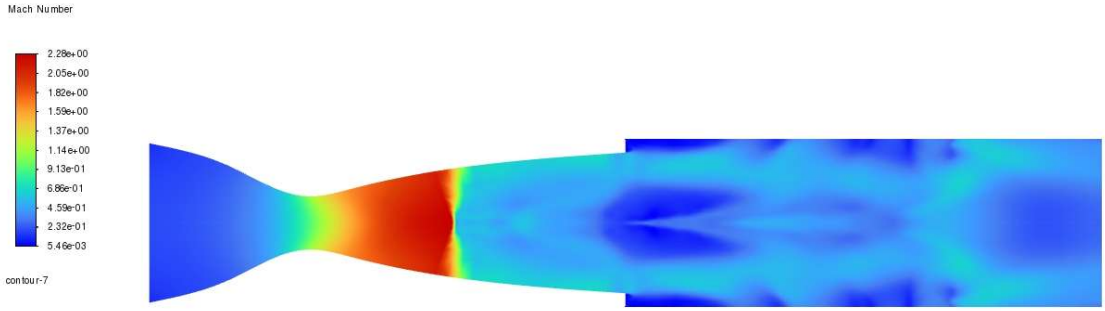

Figure 9.25 Contours of Mach Number for Expansion Wave

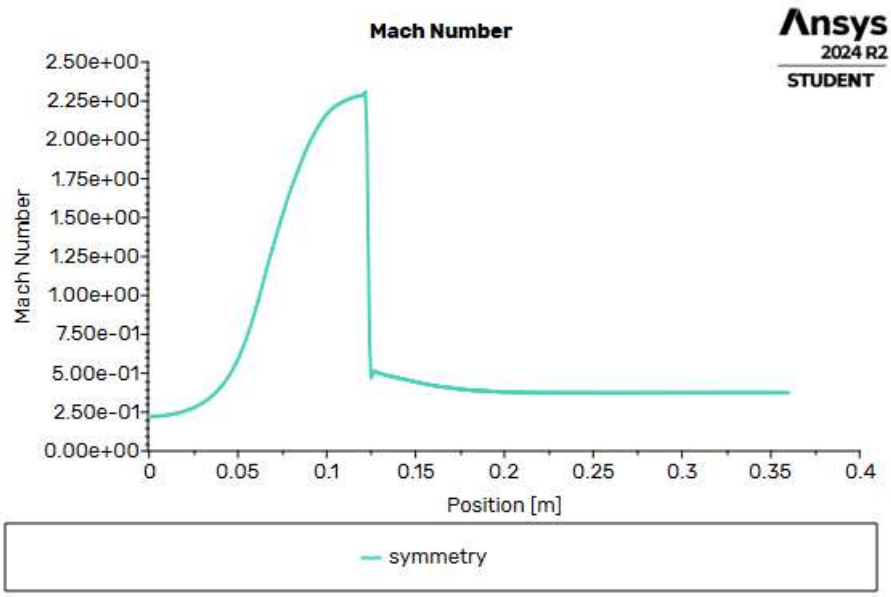

Figure 9.26 Mach Number vs Position (Expansion Wave

Static Pressure:

The diagram shows the static pressure contour within the geometry, along with a graph that plots static pressure versus position along the symmetry axis for interpretation.

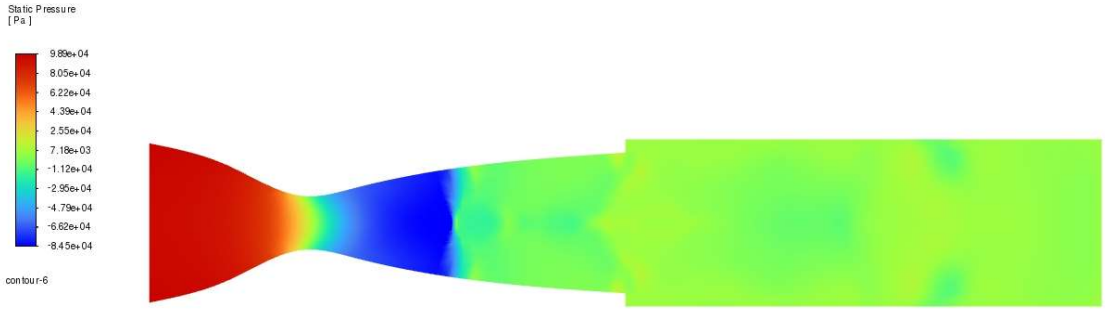

Figure 9.27 Contours of Static Pressure (Expansion wave)

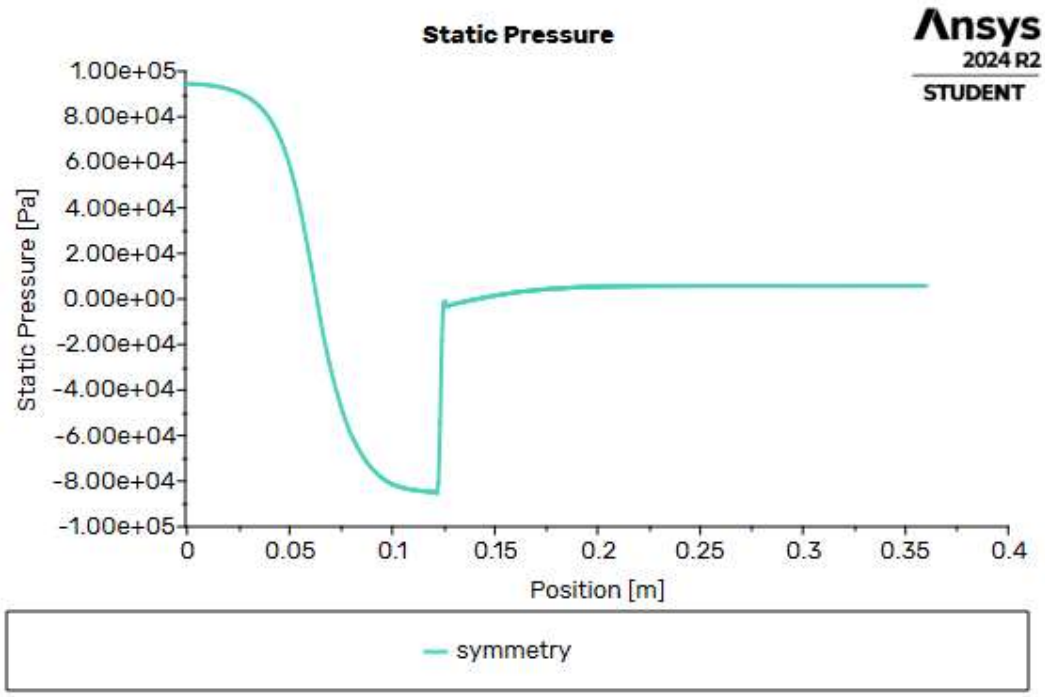

Figure 9.28 Static Pressure vs Position Graph (Expansion wave)

Static Temperature:

The figures below display the contour of static temperature across the geometry, along with a graph plotting static temperature versus position along the symmetry line for interpretation.

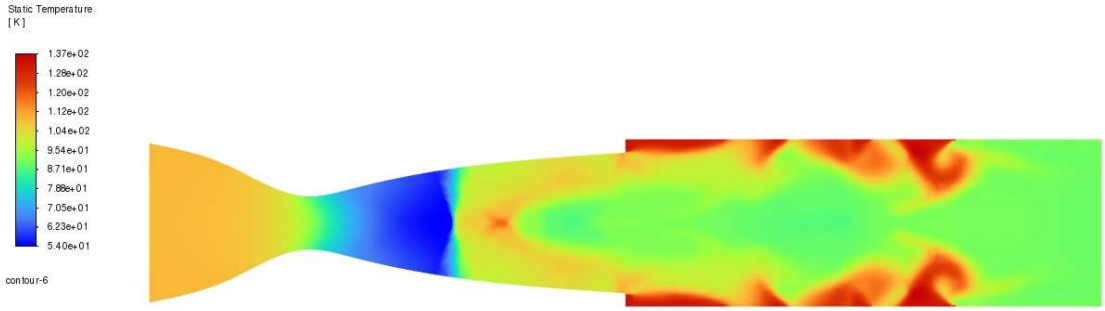

Figure 9.29 Contours of Static Temperature (Expansion wave)

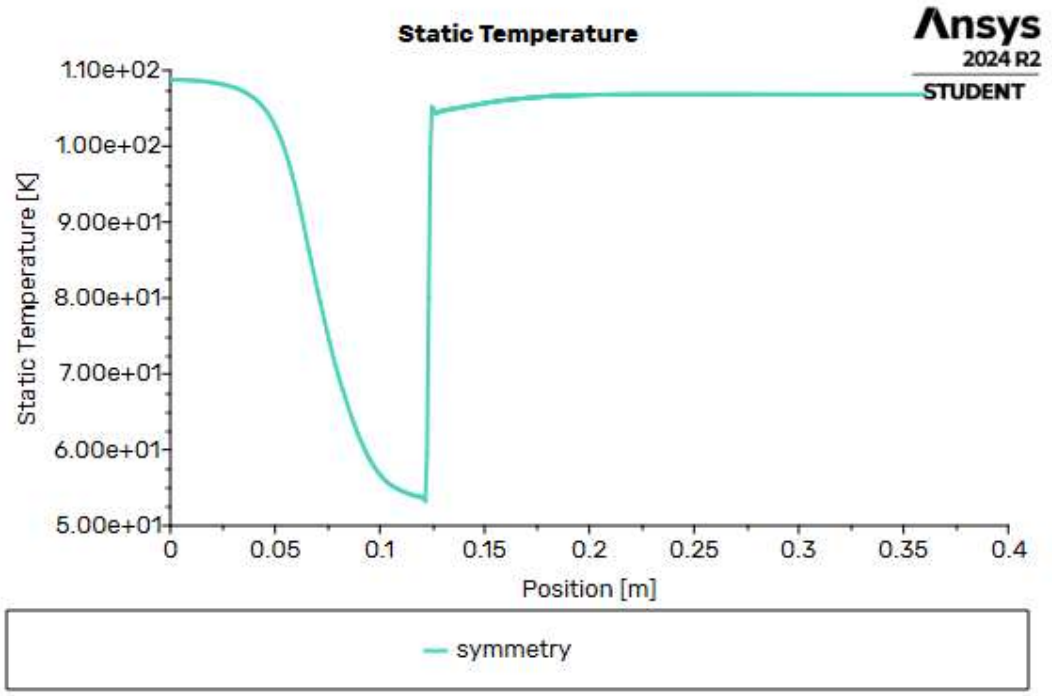

Figure 9.30 Static Temperature vs position (Expansion Wave)

Comparison:

Based on the data from calculations, the CFD results closely match the calculated conditions, with a maximum Mach number of 2.9 observed due to the expansion.

Expansion Wave			
Parameter	Analytical	CFD	Error %
	Exit	Exit	
Me	2.5	2.5217	0.9
Pe	5930.25	5722.34	3.5
Te	133.2	132.238	0.7
	After Exit	After Exit	
Mb	2.94	2.946	0.2
Pb	3000	2983.92	0.5
Tb	109.5	109.822	0.3

Table 9.5Comparison between Analytical and Simulated results (Expansion Wave)

10. KEY TAKEAWAYS AND CONCLUSION

The simulation results demonstrated a strong agreement with theoretical predictions, with only minor discrepancies observed in certain parameters. Despite these small differences, the overall trends in Mach number, static temperature, and static pressure aligned well with expected behavior, affirming the validity of the analysis. The nozzle's performance was shown to vary under different outlet conditions, as anticipated, while the fixed inlet conditions provided a stable baseline for comparison.

These variations in nozzle behavior, including the occurrence of normal and oblique shocks, expansion waves, and changes in Mach number, were consistent with the theoretical models discussed earlier. The study emphasized the critical role of back pressure in controlling flow characteristics, particularly in influencing shock formation and the expansion of flow beyond the nozzle exit.

The CFD simulations effectively captured the nozzle's response to varying operating conditions, demonstrating its capability to adapt and validating the theoretical predictions as well as the design approach.

11. REFERENCES

- Gas Dynamics by James E Johan third edition.,2006
- ANSYS, Inc. (2024). *ANSYS Fluent User's Guide* (Release 2024 R2). Canonsburg, PA: ANSYS, Inc. Retrieved from https://www.ansys.com.